

# Flow geometry variation of IGR 17091-3624 as revealed by Comptonizing Efficiency and its comparison with GRS 1915+105

Partha Sarathi Pal<sup>1</sup> and Sandip K. Chakrabarti<sup>1,2</sup>

S. N. Bose National Centre For Basic Sciences, India

Received \_\_\_\_\_; accepted \_\_\_\_\_

---

<sup>1</sup>S. N. Bose National Centre For Basic Sciences, Block JD, Sector - III, Salt Lake, Kolkata - 700098, India.

<sup>2</sup>Indian Centre For Space Physics, 43 Chalantika, Garia Station Road, Kolkata - 700084, India.

## ABSTRACT

Variability class transitions in the enigmatic black hole candidate GRS 1915+105 has been known to accompany variation of distinct flow geometry as is evidenced by the behavior of Comptonizing Efficiency (CE). This dynamical hardness ratio is defined to be the ratio between the number of power-law (hard) photons and injected seed (soft) photons and to some extent represent the geometry of the so-called Compton cloud. Similarities of light curves in some variability classes in GRS 1915+105 and IGR 17091-3624 have been reported in the literature. In the present paper, we present some more variability classes for which the light curves are similar. We examine CE variations in all these light curves of IGR 17091-3624 and find that they are also similar to what was reported for GRS 1915+105, even though masses of these objects are believed to be widely different. This shows that characterization of variability classes based on dynamical hardness ratios or CEs is likely to be black hole mass independent.

*Subject headings:* Black Holes, Accretion disk, X-rays, Radiation mechanism.

## 1. Introduction

Classifications of spectral states of neutron stars are made on the basis of color-color diagrams (CCDs) from their energetic radiations (Hasinger 1987; Hasinger & van der Klis 1989; Schulz et al. 1989). Since the masses of neutron stars fall within a narrow range, CCDs drawn using *fixed* sets of energy bands, can be used to classify all the neutron stars easily. However, stellar mass black holes are known to have masses in the range of  $3 - 20 M_{\odot}$  (Remillard & McClintock 2006) and CCDs drawn using a particular set of energy bands, may not be similar for a given spectral state. Assuming that a spectrum is fitted with multicolor black body (BB) radiation and a power-law (PL) component, the range of energy in the BB component and in PL component will change with the mass of the black hole. Energy range of BB photons for low mass blackhole could be the energy range of Comptonized photons for a high mass black hole. As a result, the same spectral state may produce different types of CCDs and just by observing CCDs one may not be able to make a statement about the spectral state (Chakrabarti 2008).

A useful hardness ratio (we hereafter call it ‘the dynamic hardness ratio’) has been defined recently Pal et al. (2011, 2013); Pal & Chakrabarti (2014). This is the Comptonizing Efficiency (CE) which is the ratio of the photon counts under the PL component and the injected BB seed photons. Of course, unlike conventional CCDs, which can be drawn without any knowledge about the spectra, CE requires the knowledge of the spectra. The added benefit is that CE provides us with the fraction of injected seed photons which are Comptonized by the hot electron cloud (Sunyaev & Titarchuk 1980, 1985). Thus, it contains information about the geometry of the Compton cloud. Its evolution with time implies the evolution of the geometry of the Compton cloud.

It has been shown recently that the variability classes of GRS 1915+105 could be characterized by average CE values which suggests that the geometry of the Compton

cloud changes systematically during variability class transitions (Pal et al. 2013). CE is very small for softer classes and larger for harder classes. Earlier, these classes were characterized by conventional CCDs for GRS 1915+105 (Morgan et al. 1997; Belloni et al. 1997a,b; Taam et al. 1997; Munro et al. 1999; Belloni et al. 2000). Since CCDs may ‘look’ different when a black hole of another mass is chosen, one may require to adjust energy ranges suitably to have similar looking CCDs for the same type of variability class. This happens while comparing IGR 17091-3624 and GRS 1915+105 (Altamirano et al. 2011a,b,c; Pahari et al. 2012). Such adjustments are arbitrary. It is thus necessary to use a mass independent concept, such as CE, i.e., a spectral state dependent dynamical hardness ratio, to check whether the two objects pass through the *same* spectral states while having similar variability class. Moreover, since the sequence of CE also gives the sequence in which the class transitions would occur, it is clearly a powerful tool to understand X-ray active black hole candidates.

IGR J17091-3624 was first observed by an INTEGRAL Galactic Center Deep Exposure Coverage (Kuulkers et al. 2003). Later, the position was confirmed through Swift observation leaving two nearby blended candidates (Kennea & Capitanio 2007; Chaty et al. 2008). In early 2011, Swift-BAT detected an outburst from IGR J17091-3624 (Krimm et al. 2011). Optical/IR observations of the compact object was performed before and during the outburst (Torres et al. 2011). In this outburst observations, radio emission was detected which confirmed the presence of an accreting black hole candidate in its low-hard state (Corbel et al. 2011; Rodriguez et al. 2011). RXTE Observations detected low-frequency quasi-periodic oscillations (Rodriguez et al. 2011) and milli-Hertz and highfrequency QPOs (Altamirano et al. 2011d; Altamirano & Belloni 2012). Again some variability classes of the light curve that were seen in GRS 1915+105 were detected for IGR 17091-3624 (Altamirano et al. 2011a,b,c; Pahari et al. 2012). As IGR J17091-3624 has lower luminosity than GRS 1915+105 (Rodriguez et al. 2011), it is assumed that IGR J17091-3624 either

consists of a very low mass black hole (Altamirano et al. 2011c) and/or it is located far away in the Galaxy with distance of around  $17 - 20$  kpc (Rodriguez et al. 2011; Altamirano et al. 2011c).

In the present paper, we show that similar variability classes of the two objects yield similar dynamical hardness ratios or CEs despite the fact that their masses could be totally different. Thus we are one step ahead of characterizing each variability class by a unique CE value, independent of the mass of the black hole. Since CEs of both IGR J17091-3624 and GRS 1915+105 are similar, the sequence in which the class transitions would take place for IGR J17091-3624 also becomes predictable. Since CE carries the information about geometry of the Compton cloud, we find that the geometry in IGR J17091-3624 evolves in the same way as that in GRS 1915+105 Pal et al. (2011, 2013); Pal & Chakrabarti (2014).

In the next Section, we present our analysis procedure and computation of Comptonizing Efficiency or CE for the IGR 17091-3624. We then present analysis results for IGR 17091-3624. Then we compare CE values of IGR 17091-3624 with CE values of GRS 1915+105 and we draw our conclusions.

## 2. Analysis & Calculation of CE

### 2.1. Spectral Analysis

We analyze RXTE-PCA and Swift-XRT data given in Table. 1. We chose data sets by common MJDs of the outbursts observation, obtained from the NASA archive for both instruments. These data are downloaded from HEASARC, NASA Archive. RXTE and Swift data are reduced with HEASOFTv6.12 software.

For RXTE data reduction, we exclude data collected for elevation angles less than  $10^\circ$ , for offset greater than  $0.02^\circ$  and those acquired during the South Atlantic Anomaly (SAA)

passage. We selected RXTE PCU2 data as it was active during the time of observation. The light curve was drawn with 2 – 40keV photons. The RXTE-PCA spectra are extracted using “standard2” mode data which have 16 sec time resolution and energy selection from 3.0 keV to 25 keV.

For Swift data reduction, the level 2 cleaned event files of SWIFT-XRT are obtained from window grade 0 events of timing (WT) mode data with xrtpipeline. From a  $40 \times 10$  pixel region in best source position spectra are extracted. The background is estimated from an off-axis region of the same size. The ancillary response files (arfs) are extracted with xrtmkarf. The WT redistribution matrix file (rmf) version (v.12) is used in the spectral fits. The Swift-XRT spectra are extracted with 16 sec time resolution and energy selection from 0.5 keV to 10 keV.

The combined 0.5 keV to 25 keV spectrum, consists of 0.5 keV to 10 keV Swift-XRT spectrum and 3.0 keV to 25 keV RXTE-PCA spectrum of the same good time interval and the same spectral resolution, are analysed for using software package XSPEC 12.8.2. Here each combined spectrum is averaged for 16 sec. Each 16 sec averaged spectra are analysed to obtain the parameters. We have used a systematic error of 0.5% for model fitting. All spectra are fitted with *diskbb* and *power-law* model along with hydrogen column density for absorption  $nH \ 1.1 \times 10^{22} cm^{-2}$  (Krimm & Kennea 2011). During fitting of all spectra we have used the technique introduced by Sobczak et al. (1999); Pal et al. (2011, 2013) to obtain spectral parameters to calculate the number of seed photons and comptonized photons. We have considered error-bars at 90% confidence level in each case.

## 2.2. Calculation of Comptonizing Efficiency (CE)

The fitting parameters are used to calculate the black body photons from the Keplerian disk and the power-law photons from the hot electron cloud. The number of black body photons are obtained from the fitted parameters of the multi-color disk black body model (Makishima et al. 1986). This is given by,

$$f(E) = \frac{8\pi}{3} r_{in}^2 \cos i \int_{T_{out}}^{T_{in}} (T/T_{in})^{-11/3} B(E, T) dT/T_{in}, \quad (1)$$

where,  $B(E, T) = \frac{E^3}{(\exp E/T - 1)}$  and  $r_{in}$  can be calculated from,

$$K = (r_{in}/(D/10kpc))^2 \cos i, \quad (2)$$

where,  $K$  is the normalization of the blackbody spectrum obtained after fitting,  $r_{in}$  is the inner radius of the accretion disk in  $km$ ,  $T_{in}$  is the temperature at  $r_{in}$  in keV,  $D$  is the distance of the compact object in kpc and  $i$  is the inclination angle of the accretion disk. Here, both the energy and the temperature are in keV. The black body flux,  $f(E)$  in photons/s/keV is integrated between 0.1 keV to the maximum energy  $dbb_e$ .  $dbb_e$  is the highest energy up to which the spectrum is fitted with diskbb model alone (Sobczak et al. 1999; Pal et al. 2011, 2013). This gives us  $N_{BB}$ , the rate of the number of the emitted black body photons.

The Comptonized photons  $N_{PL}$  that are produced due to inverse-Comptonization of the soft black body photons by ‘hot’ electrons in the Compton cloud are calculated by fitting with the power-law given below,

$$P(E) = NE^{-\alpha}, \quad (3)$$

where,  $\alpha$  is the power-law index and  $N$  is the total  $photons/s/cm^2/keV$  at 1keV. It is already reported in Titarchuk (1994), that the Comptonization spectrum will have a peak at around  $3 \times T_{in}$ . The power law equation is integrated from  $3 \times T_{in}$  to 40keV to obtain the

rate of emitted Comptonized photons. In Table. 2 we give parameters of spectral analysis of XRT and PCA spectrum.

At any given instant, the ratio  $N_{PL}/N_{BB}$  is the Comptonizing Efficiency (CE). This is a ‘hardness ratio’ but the ranges of the hard and the soft photons are automatically determined by the fitting process as described above. Thus CE is actually a dynamic hardness ratio where energy ranges were not kept fixed a priori. This way the influence of the mass of the black hole on the energy spectrum is eliminated and the results depend only on the geometry of the composite flow, having a Keplerian component for seed photons and a Compton cloud supplying hot electrons. The result is independent of the accretion flow model. It could be a two component advective flow (TCAF) (Chakrabarti & Titarchuk 1995), for instance. In this solution, the post-shock region of the low viscosity sub-Keplerian flow, namely, the CENtrifugal pressure supported BOundary Layer (CENBOL) and the associated jet behaves as the Compton cloud. The high viscosity Keplerian component on the equatorial plane supplies the seed photons.

### 3. Results

We have analysed data in the common good time intervals in which IGR 17091-3624 was observed on days mentioned in Table. 1. We compute CE for each observation. Note that in no occasion, transition from one variability class to another was observed during a single observation dwell.

We plot 2.0 – 40.0 keV RXTE-PCA light curves of 1.0 sec time bin of both IGR 17091-3624 and GRS 1915+105 in panels of Fig. 1. Several workers reported that IGR 17091-3624 sometimes shows variabilities similar to GRS 1915+105 (Altamirano et al. 2011a,b,c; Pahari et al. 2012). We show these and some more variability classes discovered



by us in Fig. 1 by plotting them side by side for comparison.

29/07/2011 observation light curve of IGR 17091-3624 resembles with the  $\mu$  class light curve of GRS 1915+105. The 24/09/2011 light curve of IGR 17091-3624 has resemblance with the  $\lambda$  class light curve of GRS 1915+105.

The 02/08/2011 observation of IGR 17091-3624 shows a similarity with the  $\kappa$  class light curve of GRS 1915+105. 10/05/2011 light curve shows a resemblance with  $\chi$  class of GRS 1915+105.

On 06/04/2011, the PCA count rate varies from 50 to 200 counts/s. The light curve matches with some part of  $\beta$  class of GRS 1915+105. Here, the value of CE varies from 0.08 % to 0.45% during softer and harder states respectively.

On 10/05/2011, the rate is steady at around 170 counts/s as in the  $\chi$  class. The object is in a hard state. A QPO at around 5 Hz is observed during this observation. Here 0.8% of soft photons interact with the Compton cloud. This remains more or less steady for the entire observation dwell.

On 20/05/2011, the rate is steady at around 170 counts/s and the light curve resembles that of the  $\chi$  class of GRS 1915+105. The object is in a hard state. A QPO at around 4 Hz is observed. Here 0.4% of soft photons are found to interact with the Compton cloud. This remains steady during the entire observation dwell.

On 17/07/2011, the rates vary in the range of 50 – 200 counts/s. This is a variable intermediate class, most likely a part of the  $\beta$  type class of GRS 1915+105, and no fixed periodicity is observed during this observation. Here, the percentage of interaction of soft photons with Compton cloud is varying from 0.04% to 0.4% during its softer and harder states respectively.

On 29/07/2011, the rate is around 300 counts/s. During this observation no quasi

periodic oscillation (QPO) is observed. Average CE is  $\sim 0.08\%$ . This class looks very similar to the  $\mu$  class of GRS 1915+105.

On 31/07/2011, the rate changes to around 150 – 350 counts/s. This light curve looks similar to  $\nu$  type variability class of GRS 1915+105. Here the flickering takes place around each 10 sec interval. Average CE varies around  $\sim 0.11\%$ . No distinct QPO is observed during this class.

On 02/08/2011, the rate remains in the range of  $\sim 100 - 200$  counts/s. The light curve shows a similar variability as in the  $\kappa$  class of GRS 1915+105. Some periodicity of  $\sim 10 - 15$  sec is observed also. The average CE is around  $\sim 0.16\%$  during this observation.

On 04/08/2011, the rate varies in the range of 200 to 350 counts/s. The light curve is variable as in  $\rho$  class of GRS 1915+105. The interval of each 'heartbeat' is around 25 sec. During this observation, around  $0.07\% - 0.2\%$  of soft photons are intercepted by the Compton cloud during their softer and harder states respectively.

On 24/09/2011, the rate varies between 100 – 500 counts/s. The light curve shows a variable shape but it does not show any regular periodicity. This can be treated to be a variable intermediate class, likely to be a part of  $\lambda$  class of GRS 1915+105. During this observation, CE is found to vary between  $0.04\%$  and  $0.2\%$  in the burst-off and burst-on states respectively.

On 22/10/2011, the rate is around 140 counts/s. In this observation also, no clear periodicity is observed. On an average,  $\sim 0.10\%$  of soft photons are intercepted by the Compton cloud similar to that in the  $\mu$  class of GRS 1915+105.

Finally, on 26/10/2011, the rate varied between 300 – 350 counts/s. This variable class also looks like the  $\mu$  class of GRS 1915+105 with no clear periodicity. In this observation, CE varies in the range of  $0.04\%$  to  $0.1\%$ .

#### 4. Discussion & Conclusion

In order to show the necessity of using CE, we first show that conventional CCDs do not look alike even when the variability class is the same for both the objects. As an example, in Fig. 2(a), we show the 2 – 40 keV data of 04/08/2011 PCA observation of IGR 17091-3624 which look similar to the so-called  $\rho$  class data of GRS 1915+105 in Fig. 2(b). In Fig. 2(d), we draw the color-color diagram of GRS 1915+105 (Fig. 2b) following Belloni et al. (2000) with 2 – 5keV, 5 – 13keV, and 13 – 60keV energy bands. When we repeat the exercise for IGR 17091-3624 (Fig. 2a) in Fig. 2(c), the CCD looks different, more like that of the  $\phi$  class. With suitable adjustment one can try to make them look similar, but this exercise is difficult to justify.

Next we plot CE variation for the 04/08/2011 observation of IGR 17091-3624 data as in Fig. 2. In Fig. 3, we plot CE as a function of time. Since spectra are necessarily from a 16s bin, CE does not show the same rise and fall as that of the light curve. However, it appears to vary around a mean. Similarly, CEs were computed for all the light curves of IGR 17091-3624 shown in Fig. 1 and the averages were computed in the largest chunk of common good time data available.

In Fig. 4, we plot average CE for IGR 17091-3624 with solid squares. Average CEs were plotted in increasing order. Dates of observations are given on the upper X-axis. For the sake of comparison, we plot average CEs of GRS 1915+105 with hollow triangles for the observed variability classes reported in Chakrabarti et al. (2005); Pal et al. (2011, 2013). CEs of GRS 1915+105 are taken from Fig. 4 of Pal et al. (2013). Shaded boxes show pairs of observations, one from IGR 17091-3624 and the other from GRS 1915+105 which were either reported to have similar looking light curves or discovered by us to be similar from the light curves presented in Fig. 1. What is observed is that the light curves are not only similar, CEs of the two black hole candidates are very close to each other on all the

occasions although their masses are widely different. In Altamirano et al. (2011c), several variability classes such  $\rho, \beta, \alpha, \mu, \nu, \lambda$  have been reported for IGR 17091-3624 on the basis of similarities of light curves with GRS 1915+105. In GRS 1915+105, these variability classes were distinguished on the basis of conventional CCDs, which, as demonstrated in Fig. 2 can be object dependent. Instead, the dynamical hardness ratios that we define and compute as CE, are found to have similar value. Several classes of light curves were not yet seen in IGR 17091-3624 (e.g., softer variability classes such as  $\phi, \delta, \gamma$  and  $\omega$ ) neither have their class transitions been observed in a single dwell. We predict that given sufficient observation time, this source would also have similar CE values in yet unseen variability classes and the same sequence in class transitions as that of GRS 1915+105 will prevail. However, given that the accretion rate in IGR 17091-3624 is perhaps much lower (Altamirano et al. 2011c), we suspect it may not show the softer variability classes.

Though the mass of IGR 17091-3624 is not known with any certainty, it is widely believed to be quite different from that of GRS 1915+105 (Altamirano et al. 2011c; Altamirano & Belloni 2012; Rao & Vadawale 2012). Even then, near equality of average CE in these two objects leads us to believe that average CE in a given class may characterize variability classes uniquely for any stellar mass black holes. Furthermore, the combined geometry of the Compton cloud and the Keplerian disk for any given variability class as given in Chakrabarti & Titarchuk (1995) should also be similarly independent of its mass. Conventional color-color diagrams with fixed energy bands, though useful to classify spectral states of neutron stars (because of very narrow range in which the mass varies) will look different for different black holes even for the same variability class of wide range of masses which they may have. This is primarily because the physical origin of photons of a given energy band is different when the mass changes.

Massive and super-massive black holes do have spectral states similar to stellar mass

black holes. They also show short and long term variabilities (e.g., Cameron et al. (2012); Emmanoulopoulos et al. (2013) and references therein). It is not unlikely that the CE defined in our method will have similar values in these objects as well. This interesting aspect will be explored separately elsewhere.

PSP Acknowledges SNBNCBS-PDRA Fellowship.

## REFERENCES

- Altamirano, D. et al. 2011a, ATel, 3230, 1
- Altamirano, D. et al. 2011b, ATel, 3299, 1
- Altamirano, D. et al. 2011c, ApJ, 742, 17
- Altamirano, D. et al. 2011d, ATel, 3225, 1
- Altamirano, D., & Belloni, T. 2012, ApJ, 747, L4
- Belloni, T., et al., 1997, ApJ, 482, 993
- Belloni, T., et al., 1997, ApJ, 488, 109
- Belloni, T., et al., 2000, A& A, 355, 271
- Chakrabarti, S. K. & Titarchuk, L. G., 1995, ApJ, 455, 623
- Chakrabarti, S. K. & Manickam, S. G., 2000, ApJ, 531, 41
- Chakrabarti, S. K. et al., 2002, ApJ, 579, 21.
- Chakrabarti, S. K. et al., 2005, A&A, 431, 825
- Chakrabarti, S. K., 2008, AIPC ,1053, 325
- Chaty, S. et al. 2008, A&A, 484, 783
- Corbel, S. et al. 2011, ATel, 3167, 1
- Cameron, D. T., et al., 2012, MNRAS, 422, 902
- Das, S. & Chakrabarti, S.K., 2004, IJMPD, 13, 1955
- Emmanoulopoulos, D., et al., 2013, MNRAS, 429, 3439

- Giri, K. & Chakrabarti, S.K., 2013, MNRAS, 430, 2836
- Hasinger, G., 1987, A&A, 186 , 153H
- Hasinger, G.; van der Klis, M., 1989, A&A, 225, 79
- Kennea, J. A. & Capitanio, F. 2007, ATel, 1140, 1
- Krimm, H. A. et al. 2011, ATel, 3144, 1
- Krimm, H. A. & Kennea, J. A. 2011, ATel, 3148, 1
- Kuulkers, E. et al. 2003, ATel, 149, 1
- Makishima, K., et al., 1986, ApJ, 308, 635
- Morgan, E. H., Remillard, R. A. & Greiner, J., 1997, ApJ, 482, 993
- Muno, M. P., Morgan, E. H. & Remillard, R. A., 1999, ApJ, 527, 321
- Pahari, M. et al., 2012, MNRAS, 422, 87
- Pal, P. S., Chakrabarti, S. K. & Nandi, A., 2011, IJMPD, 20, 2281
- Pal, P. S., Chakrabarti, S. K. & Nandi, A., 2013, AdSpR, 52, 740
- Pal, P. S. & Chakrabarti, S. K., 2014, MNRAS, 52, 740
- Rao, A. & Vadawale, S. V., 2012, ApJ, 757 12
- Remillard, R. A. & McClintock, J. E., 2006, ARA&A, 44, 49
- Rodriguez, J. et al. 2011, A&A, 533L, 4
- Schulz, N. S., Hasinger, G. & Truemper, J. 1989, A&A, 225, 48
- Sobczak, G. J. et al., 1999, ApJ, 520, 776

- Sunyaev, R. A. & Titarchuk, L. G., 1980, A&A, 86, 121
- Sunyaev, R. A. & Titarchuk, L. G., 1985, A&A, 143, 374
- Taam, E. R, Chen, X. & Swank, J. H., 1997, ApJ, 485, 83
- Titarchuk, L. G., 1994, ApJ, 434, 570
- Torres, M. A. P. et al. 2011, ATel, 3150, 1



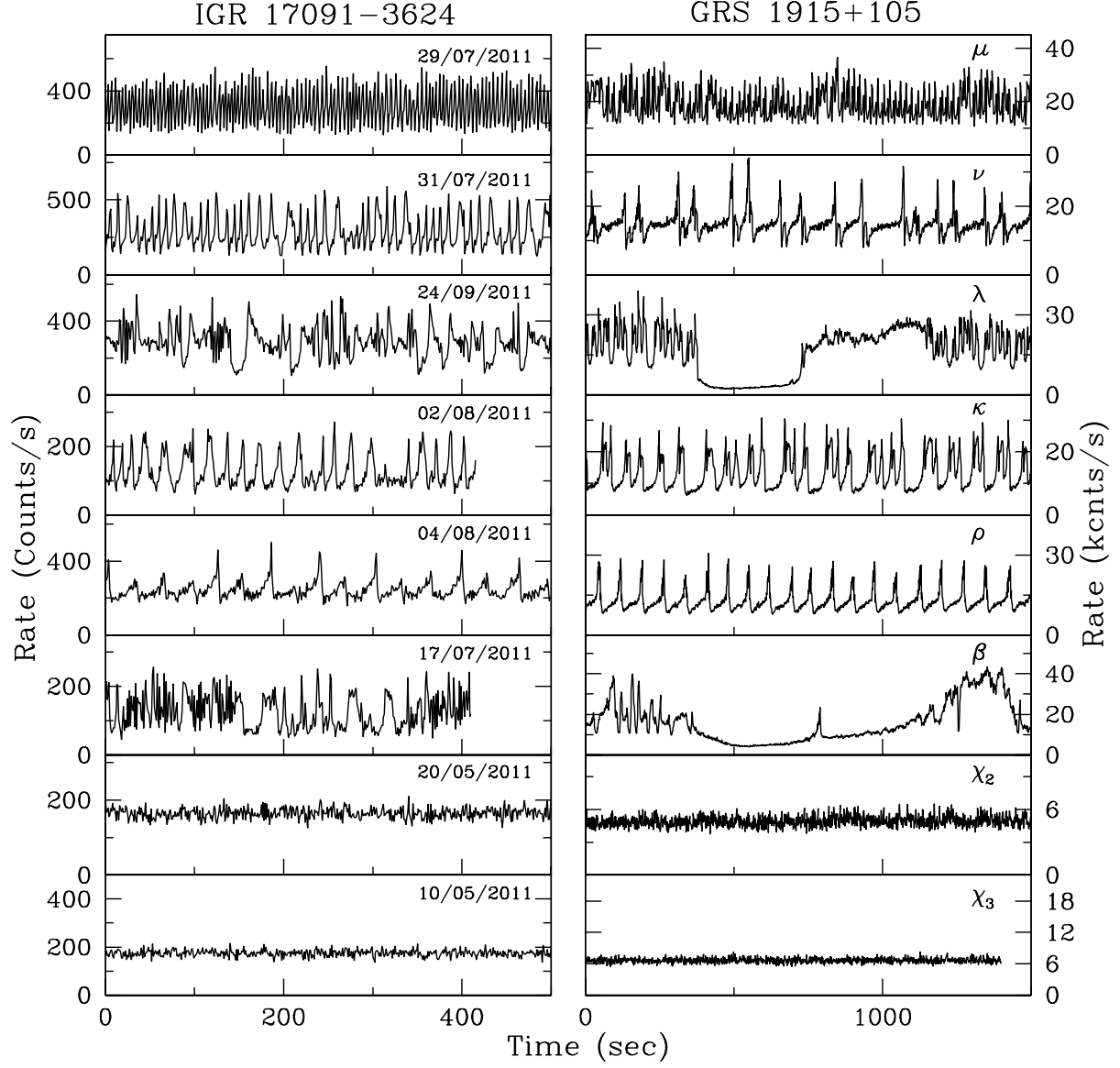


Fig. 1.— Comparison of the 2.0 - 40.0 keV 1.0 sec time bin RXTE-PCA light curves of IGR 17091-3624 (left) and GRS 1915+105 (right) to show their similarities. IGR 17091-3624 light curves clearly resemble with  $\mu$ ,  $\nu$ ,  $\lambda$ ,  $\kappa$ ,  $\rho$ ,  $\beta$ ,  $\chi_2$  and  $\chi_3$  classes of GRS 1915+105.

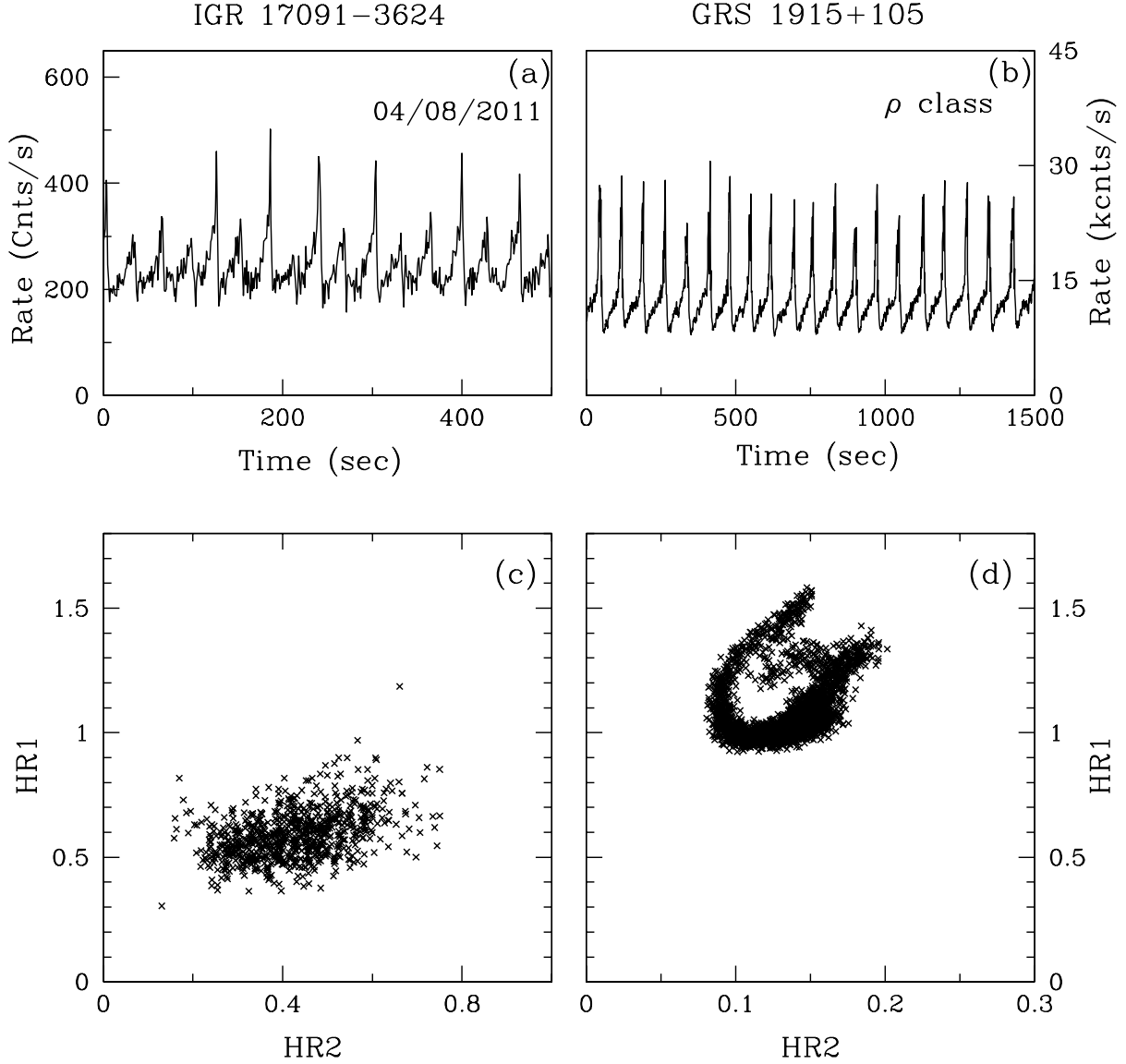


Fig. 2.— (a) 2.0 - 40 keV and 1.0 sec time bin RXTE-PCA light curve of IGR 17091-3624 of 04/08/2011 observation. (b) 2.0 - 40.0 keV and 1.0 sec time bin RXTE-PCA light curve of  $\rho$  class of GRS 1915+105. Following Belloni et al. (2000) with 2-5 keV, 5-13 keV and 13-60 keV energy bands we draw (c) Color-color diagram of (a), and (d) color-color diagram of (b). They look different indicating a totally different mass of IGR 17091-3624 as compared to that of GRS 1915+105.

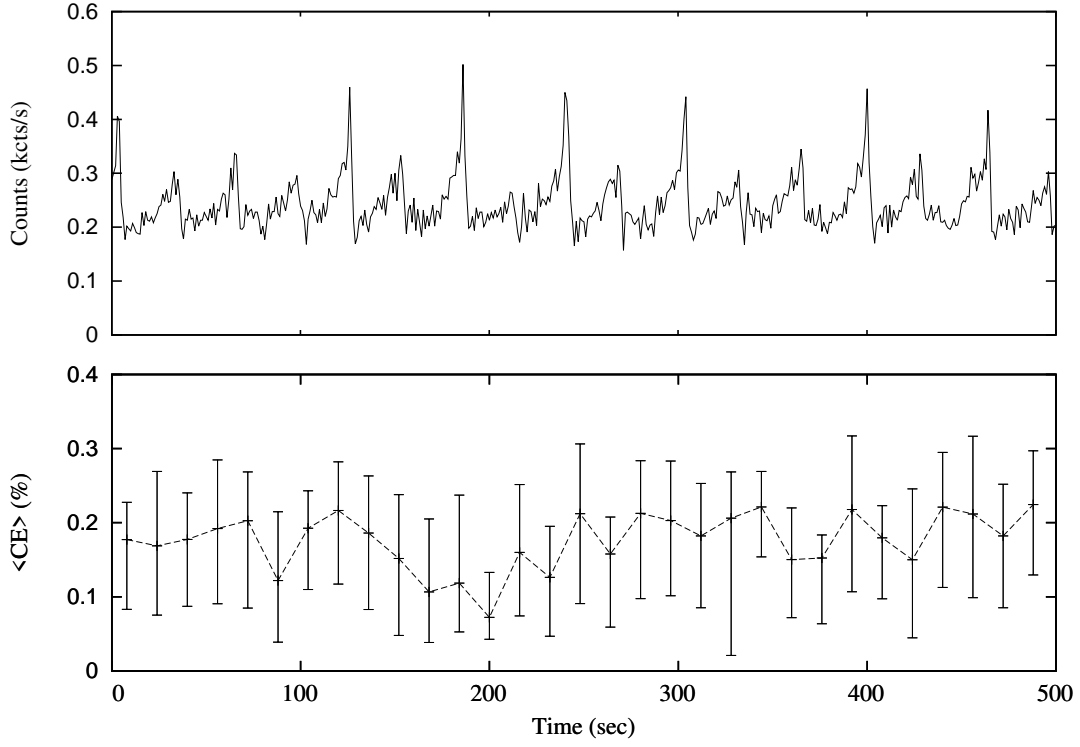


Fig. 3.— Top panel shows 2.0 - 40 keV and 1.0 sec time bin RXTE-PCA light curve of IGR 17091-3624 of 04/08/2011 observation. Bottom panel shows variation of average CE with time as obtained from 16s binned data for this observation.

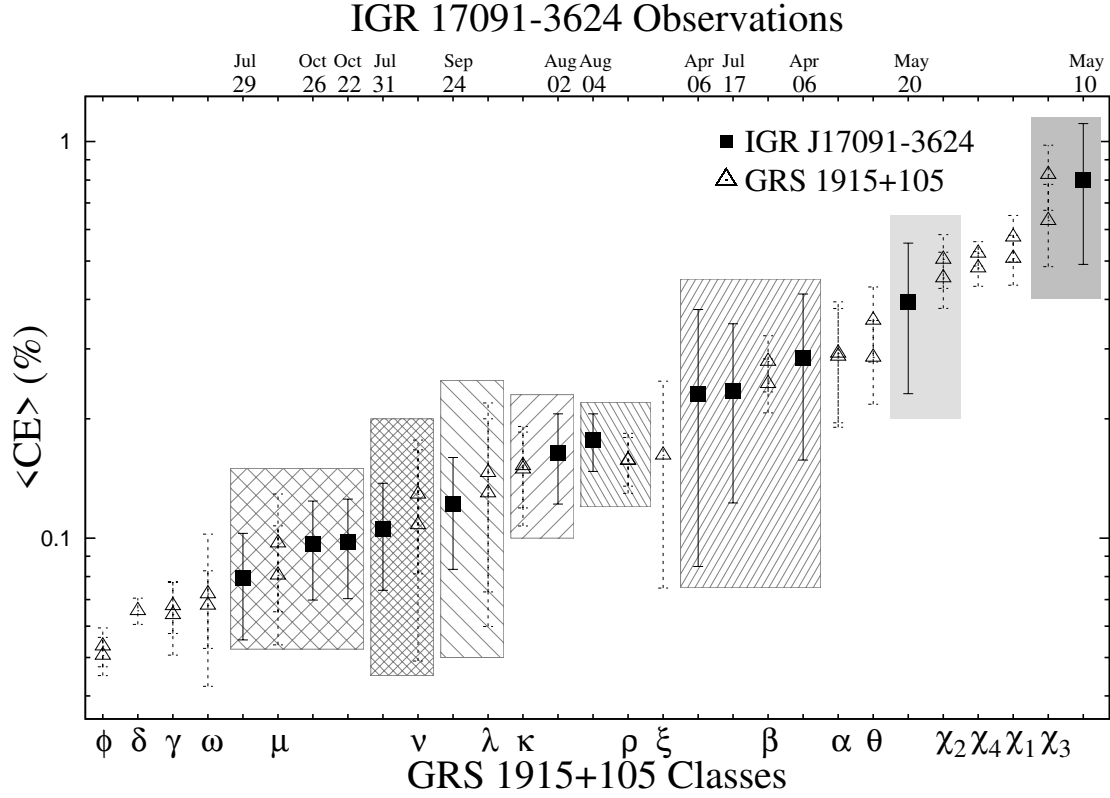


Fig. 4.— Average CE of IGR 17091-2634 (solid square) for the 2011 outburst drawn in ascending order is compared with average CE of GRS 1915+105 (hollow triangles). CE values of GRS 1915+105, are taken from the Figure. 4 of Pal et al. (2013). Error bars represent amount of excursion of average CE during these variability classes. Boxes contain CE of GRS 1915+105 and IGR 17091-3624 for which the light curves are similar. Clearly similar light curves produce similar CEs, or dynamic hardness ratios.

Table 1: Simultaneous Observation IDs along with common good time intervals of RXTE-PCA and Swift-XRT data of IGR 17091-3624 analysed in this paper.

| Observation | Swift-XRT   | RXTE-PCA       | Common GTI |
|-------------|-------------|----------------|------------|
| date        | data id     | data id        | sec        |
| 06/04/2011  | 00031921040 | 96420-01-06-03 | 461        |
| 10/05/2011  | 00031921049 | 96420-01-11-03 | 880        |
| 20/05/2011  | 00031921053 | 96420-01-13-00 | 1248       |
| 17/07/2011  | 00035096020 | 96420-01-21-02 | 411        |
| 29/07/2011  | 00035096025 | 96420-01-23-00 | 1057       |
| 31/07/2011  | 00035096026 | 96420-01-23-02 | 801        |
| 02/08/2011  | 00035096027 | 96420-01-23-04 | 454        |
| 04/08/2011  | 00035096028 | 96420-01-23-06 | 875        |
| 24/09/2011  | 00035096044 | 96420-01-31-01 | 2559       |
| 22/10/2011  | 00035096057 | 96420-01-35-00 | 552        |
| 26/10/2011  | 00035096059 | 96420-01-35-03 | 918        |

Table 2: Parameters for the spectral fits of sample simultaneous 16s bin of PCA and XRT spectra with *diskbb* plus *powerlaw* models for all observation dates.  $T_{in}$  is the black body temperature obtained from fitting.  $dbb_e$  is the upper limit of the disk blackbody spectrum. The column containing the soft photon rate contains blackbody photons in the  $0.1 - dbb_e$  keV. The column ‘power-law’ contains the power-law index  $\alpha$  obtained from fitting. The column ‘hard photons’ contains the rate at which Comptonized photons are emitted in the range  $3 \times T_{in} - 40$  keV. CE is the Comptonized Efficiency.

| Date       |   | $T_{in}$<br>(keV)      | $dbb_e$<br>(keV) | $\tilde{\chi}^2$<br>(dofs) | Soft<br>Photon<br>(kphtns/s) | Power law<br>index     | Hard<br>Photon<br>(kphtns/s) | CE<br>(%)              | $\tilde{\chi}^2$<br>(dofs) |
|------------|---|------------------------|------------------|----------------------------|------------------------------|------------------------|------------------------------|------------------------|----------------------------|
| 29/07/2011 | - | $1.66^{+0.09}_{-0.08}$ | 10               | 0.94(65)                   | $16.89^{+2.96}_{-2.47}$      | $1.95^{+0.52}_{-0.50}$ | $0.2^{+0.02}_{-0.01}$        | $0.1^{+0.02}_{-0.03}$  | 0.88(114)                  |
| 26/10/2011 | - | $1.84^{+0.12}_{-0.11}$ | 10               | 1.34(64)                   | $14.48^{+3.09}_{-2.47}$      | $2.50^{+0.50}_{-0.52}$ | $0.01^{+0.005}_{-0.002}$     | $0.07^{+0.04}_{-0.03}$ | 1.08(114)                  |
| 22/10/2011 | - | $1.97^{+0.13}_{-0.12}$ | 10               | 1.24(62)                   | $15.02^{+3.41}_{-2.68}$      | $2.15^{+0.4}_{-0.4}$   | $0.02^{+0.006}_{-0.005}$     | $0.12^{+0.07}_{-0.02}$ | 1.06(112)                  |
| 31/07/2011 | h | $1.51^{+0.09}_{-0.08}$ | 10               | 1.16(58)                   | $17.15^{+3.52}_{-2.87}$      | $2.18^{+0.33}_{-0.52}$ | $0.03^{+0.001}_{-0.006}$     | $0.15^{+0.04}_{-0.06}$ | 1.0(107)                   |
|            | s | $1.57^{+0.09}_{-0.08}$ | 10               | 0.86(57)                   | $16.19^{+3.00}_{-2.48}$      | $2.12^{+0.57}_{-0.56}$ | $0.01^{+0.003}_{-0.002}$     | $0.08^{+0.03}_{-0.02}$ | 0.78(106)                  |
| 24/09/2011 | - | $1.48^{+0.08}_{-0.08}$ | 10               | 1.35(73)                   | $20.39^{+3.73}_{-3.10}$      | $2.07^{+0.37}_{-0.72}$ | $0.03^{+0.008}_{-0.009}$     | $0.12^{+0.02}_{-0.06}$ | 1.05(123)                  |
| 02/08/2011 | h | $1.53^{+0.1}_{-0.1}$   | 10               | 1.59(54)                   | $13.82^{+3.34}_{-2.61}$      | $1.61^{+0.25}_{-0.31}$ | $0.03^{+0.002}_{-0.002}$     | $0.23^{+0.07}_{-0.06}$ | 1.02(103)                  |
|            | s | $1.56^{+0.08}_{-0.07}$ | 10               | 1.28(71)                   | $19.20^{+3.29}_{-2.75}$      | $2.30^{+0.46}_{-0.78}$ | $0.02^{+0.004}_{-0.008}$     | $0.10^{+0.04}_{-0.06}$ | 1.06(120)                  |
| 06/04/2011 | h | $1.16^{+0.10}_{-0.09}$ | 3.0              | 0.87(28)                   | $16.48^{+4.73}_{-3.60}$      | $1.49^{+0.63}_{-0.85}$ | $0.03^{+0.016}_{-0.014}$     | $0.20^{+0.15}_{-0.13}$ | 0.75(111)                  |
|            | s | $1.40^{+0.20}_{-0.11}$ | 6.0              | 1.05(40)                   | $17.46^{+4.04}_{-3.78}$      | $2.17^{+0.45}_{-0.75}$ | $0.01^{+0.004}_{-0.006}$     | $0.09^{+0.06}_{-0.05}$ | 0.86(124)                  |
| 17/07/2011 | h | $1.14^{+0.11}_{-0.09}$ | 6.0              | 1.66(23)                   | $84.59^{+15.09}_{-19.90}$    | $2.46^{+0.78}_{-0.53}$ | $0.27^{+0.050}_{-0.002}$     | $0.32^{+0.17}_{-0.08}$ | 0.79(90)                   |
|            | s | $1.87^{+0.19}_{-0.18}$ | 10               | 0.79(90)                   | $61.30^{+21.09}_{-16.55}$    | $2.98^{+0.32}_{-0.27}$ | $0.086^{+0.020}_{-0.026}$    | $0.14^{+0.04}_{-0.04}$ | 0.82(82)                   |
| 20/05/2011 | - | $1.12^{+0.21}_{-0.17}$ | 6.5              | 1.3(37)                    | $13.73^{+5.14}_{-3.54}$      | $2.19^{+0.24}_{-0.30}$ | $0.08^{+0.01}_{-0.01}$       | $0.58^{+0.29}_{-0.24}$ | 0.95(95)                   |
| 10/05/2011 | - | $1.11^{+0.26}_{-0.17}$ | 3.1              | 1.0(21)                    | $7.52^{+6.45}_{-2.96}$       | $2.02^{+0.33}_{-0.63}$ | $0.06^{+0.08}_{-0.02}$       | $0.77^{+0.37}_{-0.38}$ | 0.93(96)                   |